On the stability of a laminar incompressible boundary layer over a flexible surface

By MARTEN T. LANDAHL

Department of Aeronautics and Astronautics, Massachusetts Institute of Technology

(Received 29 November 1961)

The stability of small two-dimensional travelling-wave disturbances in an incompressible laminar boundary layer over a flexible surface is considered. By first determining the wall admittance required to maintain a wave of given wave-number and phase speed, a characteristic equation is deduced which, in the limit of zero wall flexibility, reduces to that occurring in the ordinary stability theory of Tollmien and Schlichting. The equation obtained represents a slight and probably insignificant improvement upon that given recently by Benjamin (1960). Graphical methods are developed to determine the curve of neutral stability, as well as to identify the various modes of instability classified by Benjamin as 'Class A', 'Class B', and 'Kelvin–Helmholtz' instability, respectively. Also, a method is devised whereby the optimum combination of surface effective mass, wave speed, and damping required to stabilize any given unstable Tollmien–Schlichting wave can be determined by a simple geometrical construction in the complex wall-admittance plane.

What is believed to be a complete physical explanation for the influence of an infinite flexible wall on boundary-layer stability is presented. In particular, the effect of damping in the wall is discussed at some length. The seemingly paradoxical result that damping destabilizes class A waves (i.e. waves of the Tollmien–Schlichting type) is explained by considering the related problem of flutter of an infinite panel in incompressible potential flow, for which damping has the same qualitative effect. It is shown that the class A waves are associated with a decrease of the total kinetic and elastic energy of the fluid and the wall, so that any dissipation of energy in the wall will only make the wave amplitude increase to compensate for the lowered energy level. The Kelvin–Helmholtz type of instability will occur when the effective stiffness of the panel is too low to withstand, for all values of the phase speed, the pressure forces induced on the wavy wall.

The numerical examples presented show that the increase in the critical Reynolds number that can be achieved with a wall of moderate flexibility is modest, and that some other explanation for the experimentally observed effects of a flexible wall on the friction drag must be considered.

1. Introduction

The interest in the problem arose in connexion with the publications by Krämer 1960 *a*, *b*) on the reduction of skin-friction drag obtained by covering the surface of an underwater projectile with a flexible skin of special design. Krämer's own explanation of the observed effects was that the internal friction in the flexible wall damped out the Tollmien–Schlichting waves and hence kept the boundary-layer laminar. Inspired by Krämer's work, several investigators have attacked the theoretical problem of the stability of a laminar boundary layer over a flexible surface: for example, Betchov (1959), Boggs & Tokita (1960), Hains & Price (1960), Benjamin (1960) and very recently Nonweiler (1961). Of these treatments the one by Benjamin is the most complete. He showed that when the wall is flexible there are three more or less distinct types of instability that can occur. The first type, 'Class A' waves, essentially comprises Tollmien–Schlichting waves modified by the flexible wall. The analysis showed that these waves are stabilized by a sufficient in-phase response of the flexible wall to the accompanying pressure wave, but they actually are destabilized by the presence of internal friction in the wall. The unstable waves of the second type identified by Benjamin, 'Class B' waves, are presumably similar to those induced by wind over a water surface and are stabilized by damping in the wall. The third possible kind of instability is of the Kelvin–Helmholtz type and can occur when the wall flexibility becomes large.

To act as a successful stabilizing device, a flexible wall should thus have low damping and high flexibility in order to damp out the class A waves. On the other hand, the damping must be large enough to inhibit class B waves, and the flexibility must not be so large that Kelvin–Helmholtz instability can occur. It it evident that the selection of the combination of wall parameters that will give best stabilizing results is apt to be quite critical.

In the present paper the stability theory for viscous flow over a flexible surface is examined critically in more detail. The problem is first stated as a direct boundary-layer problem by determining the admittance of the flexible wall required to maintain a given neutrally stable wave. By comparing this wall admittance to that of the given wall, a characteristic equation is obtained whose solution gives, for each wave-number, the wave speed and Reynolds number for neutrally stable waves. The characteristic equation thus obtained differs from that given by Benjamin (1960) only in that a different version of the viscous part of the solution is used, which is possibly somewhat more accurate for large wave speeds and highly curved boundary-layer velocity profiles. The characteristic equation is solved by a relatively simple graphical method similar to the original one used by Tollmien and Schlichting.

Since the flexibility of the wall introduces several types of instability, it is considerably more difficult than in the rigid-wall case to determine on which side of a neutral curve instability occurs, and a graphical method for this is therefore devised.

The problem of choosing the optimum combination of surface properties for best stabilizing results is considered next. The approach taken is that one wants to choose the Rayleigh wave speed of the surface and the internal damping so as to minimize the surface flexibility required to stabilize any wave of given wave-number. The role played by internal damping in the surface is given special attention, and a physical explanation of the different effects of damping on the class A waves, on one hand, and on the class B waves, on the other, is given. A new physical explanation of the Kelvin–Helmholtz type of instability is also presented.

Practically all the necessary mathematical analysis and most of the numerical calculations needed for the present problem have been carried out in connexion with the ordinary Tollmien–Schlichting stability theory. It is assumed that the reader is familiar with this theory as it is presented in the books by Schlichting (1960) and by Lin (1955).

2. Wall admittance for neutrally stable waves

The boundary layer is characterized by its thickness δ, non-dimensional velocity distribution $U(y)$, and Reynolds number $R = \delta U_\infty/\nu$, where U_∞ and ν are the free-stream velocity and kinematic viscosity respectively. The usual non-dimensional variables are introduced by dividing all lengths by δ, velocities by U_∞, time by δ/U_∞, and pressures by ρU_∞^2. On the steady, nearly parallel boundary-layer flow are superimposed small two-dimensional periodic disturbance velocities

$$u_1 = \psi_y, \quad v_1 = -\psi_x, \tag{1}$$

where ψ is the perturbation stream function. If we seek travelling-wave type solutions of the form

$$\psi = \phi(y)\, e^{i\alpha(x-ct)}, \tag{2}$$

where both α and c are assumed real, the differential equation for ϕ becomes the Orr–Sommerfeld equation

$$i\alpha R[(U-c)(\phi''-\alpha^2\phi)-U''\phi] = \phi^{\text{iv}}-2\alpha^2\phi''+\alpha^4\phi. \tag{3}$$

Two of the associated boundary conditions are that the perturbation velocities should vanish at infinity, i.e.

$$\phi(\infty) = \phi'(\infty) = 0, \tag{4}$$

and that (if tangential deformations of the wall are neglected) they should also give zero tangential velocity at the wall. Thus, defining the instantaneous position of the wall by

$$y = a\, e^{i\alpha(x-ct)}, \tag{5}$$

we must have

$$U+u_1 = U+\phi'\, e^{i\alpha(x-ct)} \quad \text{at} \quad y = a\, e^{i\alpha(x-ct)}. \tag{6}$$

Linearization in a gives

$$aU'_w+\phi'_w = 0, \tag{7}$$

where the subscript w refers to values at the mean position of the wall, i.e. at $y = 0$. At the wall, v_1 must be equal to the normal velocity of the wall; hence, from (1), (2) and (5) after linearization,

$$\phi_w = ca. \tag{8}$$

Combination of (7) and (8) gives

$$c\phi'_w+U'_w\phi_w = 0. \tag{9}$$

The perturbation pressure at the wall can be obtained either from the x-momentum or y-momentum equations. In the present problem the simplest procedure is, following Benjamin (1959), to integrate the y-momentum equation over y, which gives

$$\hat{p}_w = \alpha^2\int_0^\infty \left(U-c-\frac{i\alpha}{R}\right)\phi\, dy-\frac{i\alpha}{R}\phi'_w, \tag{10}$$

where

$$p_w = \hat{p}_w\, e^{i\alpha(x-ct)}. \tag{11}$$

The characteristics of the flexible surface may be expressed in several different ways. Benjamin (1960) introduced a complex compliance equal to the deflexion of the surface under a pressure wave of unit amplitude. In the present paper, we will instead let the properties of the surface be defined by its (normal) mechanical admittance

$$Y = -\frac{\text{normal velocity}}{\text{wall pressure}} = \frac{i\alpha c a}{\hat{p}_w} \tag{12}$$

to a pressure wave of given wave-number α and phase speed c. The concept of surface admittance is well known in the field of acoustics, but otherwise this choice does not have any distinct advantage over that of Benjamin. In any case, it is easy to obtain the compliance from the admittance through division by $i\alpha c$. The admittance defined by (12) is non-dimensional and related to the dimensional admittance Y_* through

$$Y = \rho U_\infty Y_*. \tag{13}$$

The non-dimensional admittance Y_0 required to maintain neutrally stable travelling waves is obtained from (12), (8) and (10): thus

$$Y_0 = i\alpha\phi_w \bigg/ \left[\alpha^2 \int_0^\infty (U - c - i\alpha/R)\,\phi\, dy - i\alpha\phi'_w/R\right]. \tag{14}$$

The problem is now reduced to that of finding solutions of (3) for real α and c which satisfy (4) and (9). By solving for the fourth boundary condition (14), we have cast the original problem as a direct boundary-value problem and thus deferred the characteristic value problem to a later stage. This technique might possibly be used to advantage also in other stability problems.

3. Asymptotic solution for large Reynolds number

As in the rigid-wall case, the Reynolds number for neutral stability may be expected to be relatively large, so that the same asymptotic technique may be employed. Thus two asymptotic solutions ϕ_1 and ϕ_2 of (3) are obtained from the 'inviscid' equation

$$(U-c)(\phi'' - \alpha^2\phi) - U''\phi = 0. \tag{15}$$

The inviscid solutions were given by Heisenberg in the form of a convergent series in α^2 (see Lin 1955, p. 34). We will denote the linear combination of ϕ_1 and ϕ_2 that vanishes at infinity by Φ.

A second pair of asymptotic solutions are the 'viscous' solutions ϕ_3 and ϕ_4 obtained as the leading term of an expansion in $(\alpha R)^{-\frac{1}{3}}$. The solution vanishing at $y = \infty$ is the one commonly denoted by ϕ_3 and given by (e.g. see Lin 1955, p. 128)

$$\phi_3 = \left(\frac{\zeta}{U-c}\right)^{\frac{5}{4}} \int_\infty^\zeta d\zeta \int_\infty^\zeta d\zeta\, \zeta^{\frac{1}{2}} H_{\frac{1}{3}}^{(1)}\left[\tfrac{2}{3}(i\zeta)^{\frac{3}{2}}\right], \tag{16}$$

where

$$\zeta = (\alpha R)^{\frac{1}{3}} \left[\frac{3}{2}\int_{y_c}^{y} (U-c)^{\frac{1}{2}}\, dy\right]^{\frac{2}{3}}. \tag{17}$$

We have here used the improved solution given by Tollmien (1947) which is uniformly valid for all y. The reason for this is twofold. First, the values of c encountered in the flexible-wall problem can be quite high, so that the profile curvature at the critical point may be comparatively large. Secondly, the values of λ calculated according to (21) are generally much smaller than those obtained using the simpler definition of λ (cf. Lin 1955, equation (3.6.6)) so that the correction for large c is much less. The rule for selecting the correct branches of the solutions is always to pass below the critical point y_c (defined by $U(y_c) = c$) for nearly real values of c and positive U'_w (see Lin 1955, p. 35).

The proper solution satisfying (4) and (9) is thus

$$\phi = \Phi - \phi_3(c\Phi'_w + U'_w \Phi_w)/(c\phi'_{3w} + U'_w \phi_{3w}). \tag{18}$$

In evaluating the pressure at the surface, it was shown by Benjamin (1959) that a very good approximation to (10) is

$$\hat{p}_w \simeq \alpha^2 \int_0^\infty (U-c)\,\Phi\, dy = c\Phi'_w + U'_w \Phi_w, \tag{19}$$

where (15) has been used. The error in (19) is at most of order $(\alpha R)^{-\frac{1}{3}}$ and can therefore be neglected in consistency with the asymptotic expansion sought.†

Setting

$$U'_w \phi_{3w}/c\phi'_{3w} = -(1+\lambda)\,F(z), \tag{20}$$

where

$$\lambda = \frac{U'_w}{c^{\frac{3}{2}}}\left[\frac{3}{2}\int_0^{y_c}(c-U)^{\frac{1}{2}}\,dy\right] - 1, \tag{21}$$

$$z = (\alpha R)^{\frac{1}{3}}\left[\frac{3}{2}\int_0^{y_c}(c-U)^{\frac{1}{2}}\,dy\right]^{\frac{2}{3}}, \tag{22}$$

and $F(z)$ is the Tietjens function defined by

$$F(z) = -\frac{\int_\infty^{-z} d\zeta \int_\infty^{\zeta} \zeta^{\frac{1}{2}} H^{(1)}_{\frac{1}{3}}[\tfrac{2}{3}(i\zeta)^{\frac{3}{2}}]\,d\zeta}{z\int_\infty^{-z} \zeta^{\frac{1}{2}} H^{(1)}_{\frac{1}{3}}[\tfrac{2}{3}(i\zeta)^{\frac{3}{2}}]\,d\zeta}, \tag{23}$$

we obtain from (18), neglecting terms of order $(\alpha R)^{-\frac{1}{3}}$ arising from the factor $[\zeta/(U-c)]^{\frac{1}{4}}$ in (16),

$$\phi_w = \Phi_w + (1+\lambda)\,F(z)\,[\Phi_w + (c/U'_w)\,\Phi'_w]/[1-(1+\lambda)\,F(z)]. \tag{24}$$

Equations (19) and (24) may now be substituted into (14) to give Y_0. The result simplifies considerably if, following Lin, we introduce the related functions

$$\mathscr{F}(z) = [1-F(z)]^{-1}, \tag{25}$$

and

$$u + iv = [1 + U'_w \Phi_w/c\Phi'_w]^{-1}. \tag{26}$$

A comprehensive table of $\mathscr{F}$ has recently been given by Miles (1960). The imaginary part of (26) is very nearly a function of c alone, tables of which have been given by Lin (1945) and by Lees (1947). For small α, the real part is approximately

$$u \simeq cU'_w/\alpha(1-c)^2. \tag{27}$$

† If instead the x-momentum equation is used to calculate the pressure a result is obtained that differs slightly from (19) by terms involving $\lambda(c)$. The precise reason for this difference has not yet been found. However, it has been pointed out to me by Dr T. Brooke Benjamin that in an approximate theory the use of the y-momentum equation is likely to give a more accurate result.

Substituting (25) and (26) into (19) and (24), and then finally into (14), we arrive at the wall admittance required to maintain neutrally stable waves:

$$Y_0 = -\frac{i\alpha}{U'_w}\left[u+iv-\frac{\mathscr{F}}{1+\lambda(1-\mathscr{F})}\right]. \tag{28}$$

For the Blasius profile, λ is less than 0·05 for $c \leqslant 0{\cdot}7$. Also z differs from $(\alpha R)^{\frac{1}{3}} cU_w'^{-\frac{2}{3}}$ by less than 3 % for $c \leqslant 0{\cdot}7$. Apparently a good approximation for most practical cases is to neglect λ and use the simplified expression (32) for z, as was done by Benjamin (1960).

4. The eigenvalue problem

For a flexible wall with a surface admittance given as a function of wave-number and wave speed, there exist certain combinations of α, c and R for which neutrally stable travelling waves are possible. These eigenvalues are determined by

$$\Delta Y = Y_0 - Y = 0. \tag{29}$$

The introduction of Y_0 from (28) gives the characteristic equation

$$-\frac{i\alpha}{U'_w}\left[u+iv-\frac{\mathscr{F}}{1+\lambda(1-\mathscr{F})}\right] - Y = 0. \tag{30}$$

For low to moderately large values of c, λ may be neglected, whereby (30) simplifies to

$$\mathscr{F} - u - iv + iU'_w Y/\alpha = 0, \tag{31}$$

with

$$z = c(\alpha R)^{\frac{1}{3}}/U_w'^{\frac{2}{3}}. \tag{32}$$

This equation is identical to that given by Benjamin (1960). As the subsequent results will show, the unstable waves tend to have a higher wave speed for a flexible surface with damping than for a rigid one, so that the difference between (30) and (31) might in extreme cases be of importance. However, in all the numerical examples given below, the simplified equation (31) has been used.

To solve (30) it is convenient to recast it as follows:

$$\mathscr{F}(z) = \frac{(1+\lambda)\,\{(U'_w/i\alpha)\,Y+u+iv\}}{1+\lambda\{(U'_w/i\alpha)\,Y+u+iv\}} = G(\alpha, c). \tag{33}$$

In this way the Reynolds number enters directly only into the left-hand side of the equation through the parameter z. The complex function $\mathscr{F}$ may be plotted in a Argand diagram with z as a parameter. This is done in figure 1 using the table of $\mathscr{F}(z)$ given by Miles (1960). For a graphical solution of (33) the right-hand side $G(\alpha, c)$ may be plotted for each α with c as a parameter in the same polar diagram as $\mathscr{F}$. The intersections of the curves give the eigenvalues c and z, and hence R, for each α. The procedure is an extension of the original method proposed by Tollmien and Schlichting (see Schlichting 1960, pp. 394–396).

As a representation of the flexible wall in the calculations that follow, the expression corresponding to that suggested by Benjamin (1960) will be used.

This is the expression valid for non-dispersive systems such as a membrane with frictional damping, or for a deep layer of uniform elastic material, viz.

$$Y = -\frac{ic}{m\alpha(c_0^2 - c^2 - icd/\alpha)}, \tag{34}$$

where $m = m^*/\rho\delta$, $c_0^2 = T^*/m^*U_\infty^2$, $d = d^*\delta/U_\infty$ are the non-dimensional effective mass, Rayleigh-wave speed, and damping, respectively. By letting these quantities vary with α we may also use this expression to represent dispersive systems. For a visco-elastic material like rubber, the parameters are actually

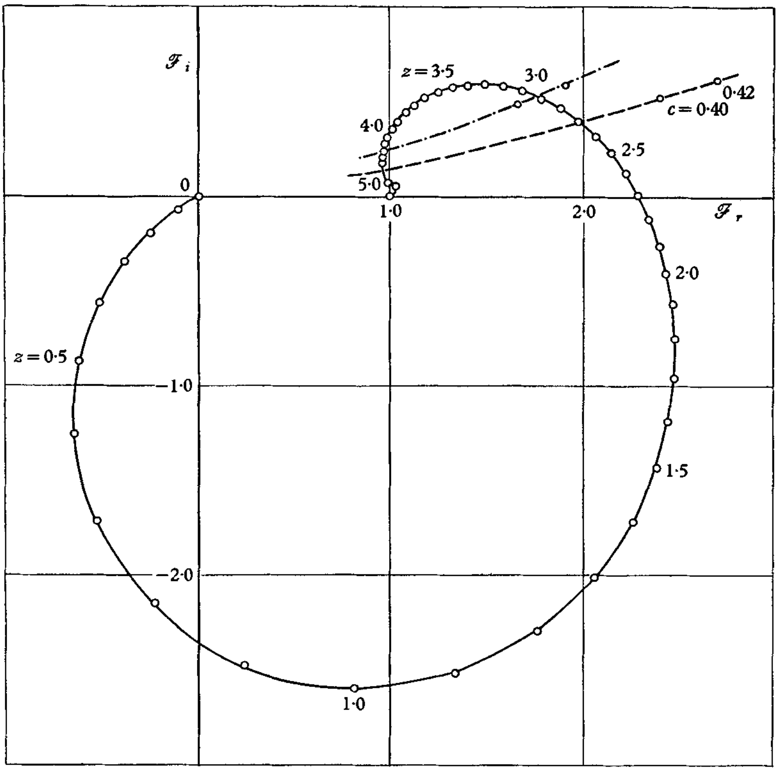

FIGURE 1. The function $\mathcal{F}$. The sample G-curves correspond to $\alpha = 0{\cdot}8$ and the flexible wall considered in figure 4. (—·—·—, Flexible wall; ––––, rigid wall.)

also (complex) functions of the frequency, i.e. of αc, due to relaxation effects in the material. However, (34) probably reproduces reasonably well the behaviour of any elastic surface for c close to c_0. As will be apparent in later sections, this region is of particular interest in the present problem. For very large wavelengths and low wave-velocities, the stiffness of the surface must approach a constant value; hence mc_0^2 must vary as α^{-2} for low α. The flexible skin developed by Krämer (1960 *a*, *b*) consisted of an outer rubber skin attached to a rigid surface through short stubs. The space between the outer skin and the rigid surface was filled with a viscous liquid. For large wavelengths, the spring constant of such a wall is determined mainly by the stubs. Also, the mass reaction term is then dominated by the inertia of the fluid sloshing back and forth due to the wavy deformation, and a simplified analysis similar to that of Krämer (1960*b*) shows that in the limit of vanishing α the properties of the layer are given by (34) with m proportional to α^{-2} and c_0 and d constant. For large α

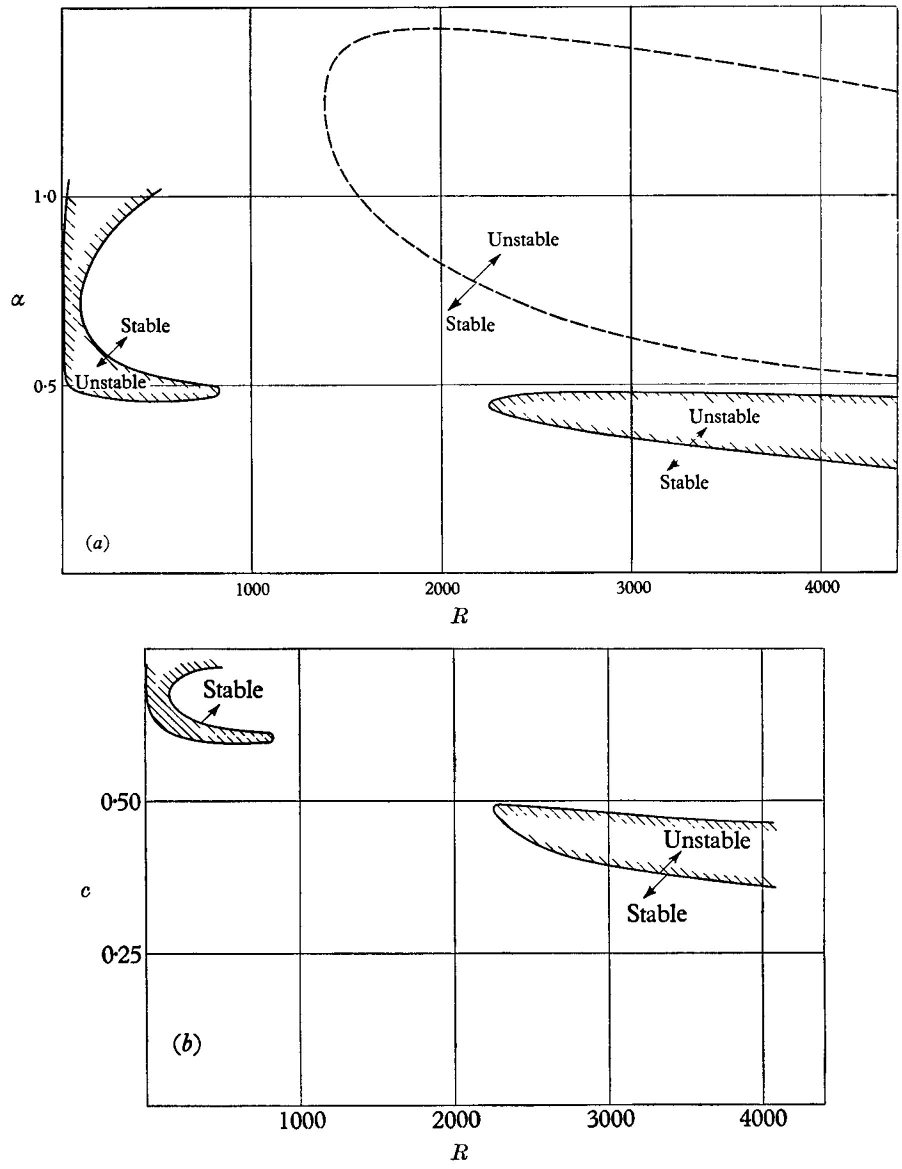

FIGURE 2. Curves of neutral stability for a flexible wall with $c_0 = 0{\cdot}75$ and $d = 0{\cdot}025$. $m = 2$ for $\alpha \geqslant 0{\cdot}5$, $m = 0{\cdot}5\alpha^{-2}$ for $\alpha \leqslant 0{\cdot}5$: (*a*) wave-number (——, flexible wall; – – – –, rigid wall). (*b*) Wave speed.

the surface would behave more like a membrane or plate. In the numerical examples shown in figures 2, 3 and 4, the properties of a flexible wall of Krämer's type are simulated approximately by letting m be constant for α larger than a certain value α_0, and proportional to α^{-2} for $\alpha < \alpha_0$. The other parameters are taken to be constants. Although this is a very crude approximation to the properties of this particular kind of flexible wall, it probably will reproduce qualitatively the main effects. In all the numerical examples, m was set equal to 2 for

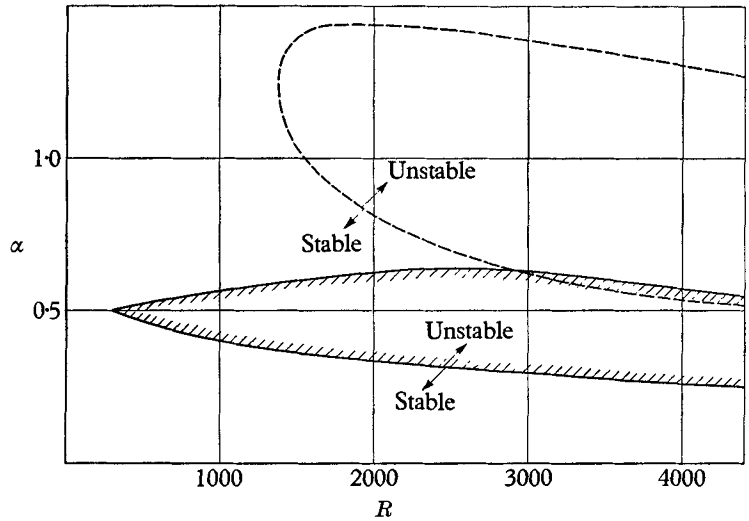

FIGURE 3. Curve of neutral stability for a flexible wall with $d = 0{\cdot}05$. c_0 and m the same as in figure 2. ——, Flexible wall; – – – –, rigid wall.

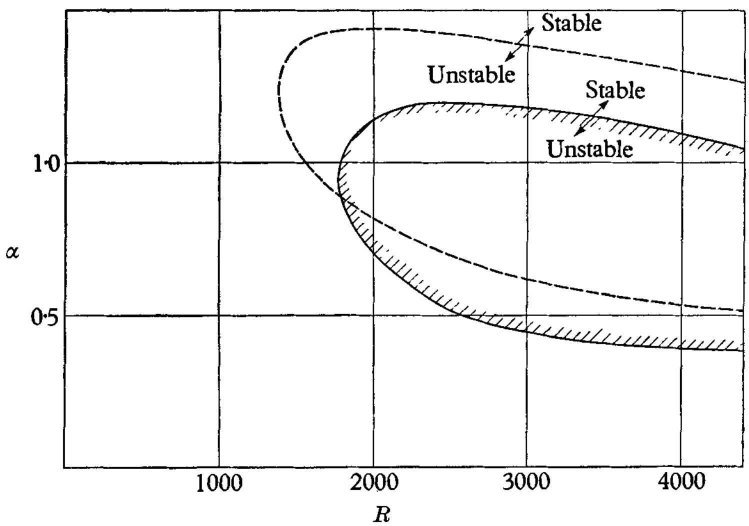

FIGURE 4. Curve of neutral stability for a wall with $d = 0{\cdot}05$ and $c_0 = 1$. m the same as in figures 2 and 3. ——, Flexible wall; – – – –, rigid wall.

$\alpha \geqslant 0{\cdot}5$ and equal to $0{\cdot}5\alpha^{-2}$ for $\alpha \leqslant 0{\cdot}5$. In the calculations, u was approximated by the first two terms of a power series expansion in α, the leading term which is proportional to α^{-1} being the same as (27). Values of v for $c > 0{\cdot}5$ were obtained from the well-known approximate formulae (Lin 1955, equation (5.4.2)) using auxiliary tables given by Lees (1947). It should be noted that, for some of the cases considered here, values of $(\alpha R)^{-\frac{1}{3}}$ and c were encountered which are clearly beyond the limits of applicability of the ordinary approximate theories, and the accuracy of the calculations should be assessed accordingly. In particular, the low-Reynolds-number loops in figure 2 should be regarded as only qualitatively correct.

The examples shown in figures 2, 3 and 4 were chosen to demonstrate the influence of varying c_0 and d. Figure 2 has $c_0 = 0{\cdot}75$ and a low damping, $d = 0{\cdot}025$. Wave-numbers for neutral stability are shown in figure 2*a* and corresponding wave speeds in figure 2*b*. Two stability loops appear, one roughly corresponding to the one for the rigid-wall case (which is included for comparison), and another one at rather low Reynolds numbers. (A method to determine which side of the neutral curve represents instability is given in the following section.) The loop at lower Reynolds number is very sensitive to changes in the damping. If the damping is increased, the unstable region enclosed by this loop will decrease. As shown in figure 3, the lower loop has vanished completely for $d = 0{\cdot}05$. If the damping is decreased, on the other hand, the loop will expand and eventually merge with the upper loop, so that some wave-numbers will be unstable for all Reynolds numbers. It will be apparent below that the unstable waves within the lower loop are of class B type according to Benjamin's classification (1960). The upper loop, on the other hand, is affected in the completely opposite manner by the damping, as becomes evident by comparing figures 2 and 3. The unstable waves in the upper loop are of the class A type. A physical explanation for the different effects of damping in the two cases is given later. For the combination of surface parameters used in figure 3, the critical Reynolds number is considerably lower than in the rigid-wall case, although the range of unstable wave-numbers is substantially smaller. An increase in the critical Reynolds number in this case can be obtained by increasing the surface stiffness, i.e. by increasing c_0. With $c_0 = 1$, which is the case shown in figure 4, the critical Reynolds number is slightly higher than in the rigid-wall case, but the range of unstable wave-numbers is larger than in the case shown in figure 3. This indicates that if one parameter is given, say m, there is for every α an optimum combination of the other two that makes the boundary layer stable for as high a Reynolds number as possible. This line will be explored in a later section. We note that, in the examples shown, the beneficial effects on the critical Reynolds number are rather modest despite the rather high surface flexibility chosen. For the case considered in figure 4, the flexibility is such that the deformation of the wall due to a steady constant pressure equal to the dynamic pressure is equal to the boundary-layer thickness, i.e. the flexibility is moderately large.

5. Determining the unstable regions

The procedure described above for calculating the neutral curve gives, of course, no direct information about whether disturbances of a certain wavelength are stable or unstable for a particular Reynolds number. As the use of any standard method like the Nyquist diagram is not feasible to determine this in the present problem, an approximate method has instead been developed based on the fact that the eigenvalues are mostly located very close to the real axis.

Consider the imaginary part of the function ΔY (equation (29)) plotted versus the real part with c as a parameter for a given combination of α and R. Near a simple zero $c = c_e$ (an eigenvalue), the function will behave like

$$\Delta Y = f(c)\,(c - c_e), \tag{35}$$

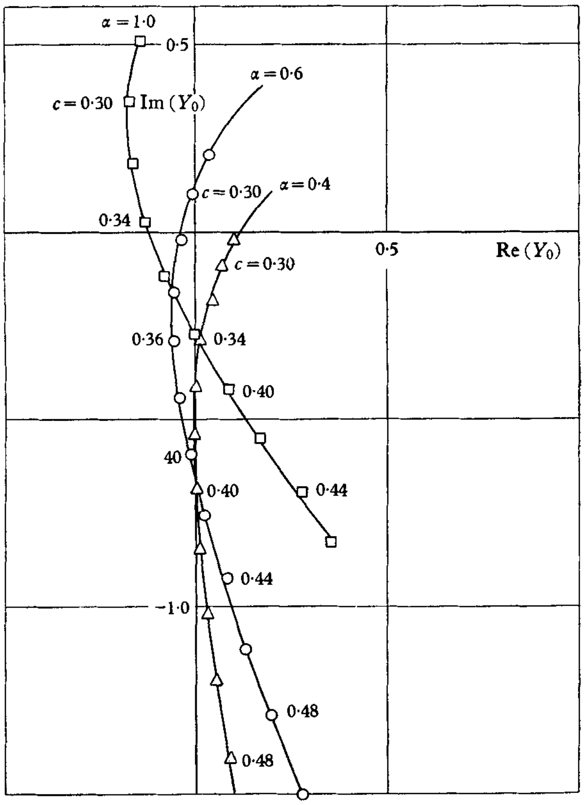

FIGURE 5. 'Fluid admittance' Y_0 for $R = 4000$ and various values of α.

where $f(c)$ varies so slowly that it can be considered constant in a small region around c_e. If c_e is purely real, ΔY will pass through the origin. If the imaginary part of $c_e = c_{er} + ic_{ei}$ is positive (an unstable root), the vector ΔY will rotate counterclockwise an angle of π as c_{er} is passed (c increasing). Hence there is an unstable root whenever the curve for ΔY passes (close) to the right of the origin. To the first order, the amplification rate is given by

$$ic_{ei} = -\left(\Delta Y \Big/ \frac{\partial \Delta Y}{\partial c}\right)_{c=c_{er}}. \tag{36}$$

(This expression is purely imaginary since ΔY is perpendicular to $\partial \Delta Y/\partial c$ for minimum $|\Delta Y|$.)

As an illustration we consider the rigid-wall case for which $\Delta Y = Y_0$. Figure 5 shows Y_0 for $R = 4000$ and various values of α. It is seen that disturbances with $\alpha = 0{\cdot}6$ and $1{\cdot}0$ are unstable, whereas $\alpha = 0{\cdot}4$ is stable. Some preliminary estimates indicate that the most unstable wave for this Reynolds number is approximately that with $\alpha = 1$, for which (36) gives

$$c_e = 0{\cdot}351 + 0{\cdot}016i,$$

is reasonably good agreement with calculations previously given in the literature.

The method fails in two specific circumstances. If the wave speed c_0 for the flexible skin is near an eigenvalue (which might happen in case of class B waves), ΔY will rotate counterclockwise an angle π as c_0 is passed since Y has a pole at approximately $c = c_0 - id/2\alpha$. To avoid this difficulty, one can instead of ΔY consider the function E defined by

$$E = (Y_0/Y) - 1, \tag{37}$$

which has no poles near the real axis. Using the expressions (28) and (34) for Y_0 and Y, we obtain

$$E = \frac{m\alpha^2}{U'_w}\left(\frac{c_0^2}{c} - c - \frac{id}{\alpha}\right)\left[u + iv - \frac{\mathscr{F}}{1+\lambda(1-\mathscr{F})}\right] - 1. \tag{38}$$

The function E can be investigated in the same way as ΔY.

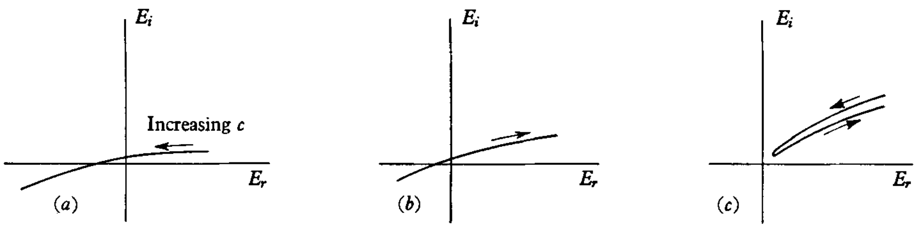

FIGURE 6. Illustration of the use of the function E to determine whether instability occurs for a given α and R. (*a*) Unstable class B wave; (*b*) stable class A wave; (*c*) Kelvin–Helmholtz instability.

A second difficulty arises when two roots are located very close together or are complex conjugates, or very nearly so. This happens in the case of Kelvin–Helmholtz instability. Benjamin's (1960) investigation of this type of instability was based on a simplified second-order equation. In the complete problem the roots rarely occur in complex conjugate pairs, except in the region of small α for large flexibility and in other special cases. A method to construct such cases is given in the next section. However, it may often happen that two roots are very nearly complex conjugates. If there are two roots c_1 and c_2 located very close together, the function E will, in the neighbourhood of these roots, behave like

$$E = (c - c_1)(c - c_2)\, q(c), \tag{39}$$

$q(c)$ being a slowly varying function. Hence E may not rotate as c passes c_1 and c_2, and the above method will be unable to determine whether there is an unstable root. However, this case of instability may be detected by considering the derivative of E:

$$\frac{\partial E}{\partial c} = (c - c_1)(c - c_2)\frac{\partial q}{\partial c} - (c_1 + c_2 - 2c)\, q \simeq 2\left(c - \frac{c_1 + c_2}{2}\right) q, \tag{40}$$

which rotates an angle of π or $-\pi$ depending on whether the unstable or the stable root is farther from the real axis. The various cases that can occur are illustrated in figure 6.

In most practical cases one can determine the unstable wavelengths directly from the complex $\mathscr{F}$-diagram used in the previous section to determine the neutral curve.

6. Optimum surface properties for boundary-layer stabilization

Benjamin (1960) found that for a flexible surface to be effective as a stabilizing device its admittance should generally have a large negative imaginary part and as small a real part as possible. (The real part of Y is always positive for positive damping.) This result is evident from the graphical construction for finding the neutral curve (see figure 1). A negative imaginary part of Y will displace the G-curve for a given α to the left (see equation (33)), making the unstable region of z (the region on the $\mathscr{F}$-curve above the G-curve) smaller, i.e. the region of unstable Reynolds number smaller. A positive real part of Y, on the other hand, will displace the curve downward, making the unstable region of z larger.

To make the imaginary part of Y a large negative number, one could either make m small or c_0 close to (but always larger) than the wave speed of the unstable Tollmien–Schlichting waves (cf. equation (34)). For c close to c_0, on the other hand, the real part of Y will become large and this will have a destabilizing effect. Since m is proportional to the ratio of the mass of flexible layer to the mass of the fluid within the boundary layer, there will in practice be a lower limit on the value of m one can obtain. The practical problem is thus to choose c_0 and d in such a way as to allow as large a value of m as possible. The introduction of (34) into the characteristic equation (29) gives

$$Y_0 + \frac{ic}{m\alpha(c_0^2 - c^2 - icd/\alpha)} = 0. \tag{41}$$

The first term has a root at $c = c_T = c_{Tr} + ic_{Ti}$, where c_T is the complex wave speed for an unstable Tollmien–Schlichting wave. The second term has a pole at $c = c_1 \simeq c_0 - id/2\alpha$. Expanding in series about these points and retaining only the linear term in each, we obtain

$$A(c - c_T) + \{m(c - c_1)\}^{-1} = 0, \tag{42}$$

where
$$A = 2\alpha i(\partial Y_0/\partial c)_{c=c_{Tr}} = A_r + iA_i. \tag{43}$$

Usually A_r and A_i are positive, with $A_i \ll A_r$ (see figure 5). The approximation (42) is generally good for large values of m when the modification of the eigenvalue due to the flexible wall is small, and when d is very small. For a given α, one wants to choose the parameters m, c_0 and d so that both roots of (42) are stable, i.e. are located in the lower half-plane. In the limiting case at least one of the roots is located on the real axis, say at $c = a$. The second root $c = b$ will then be located at

$$b = c_T + c_1 - a = b_r + ib_i, \tag{44}$$

where
$$b_r = c_{Tr} + c_0 - a, \quad b_i = c_{Ti} - \epsilon, \quad \epsilon = d/2\alpha. \tag{45}$$

Solving (42) for c_1 in terms of a, we obtain

$$c_1 = a + B/m(a - c_T), \tag{46}$$

where $B = A^{-1} = B_r - iB_i$. Hence

$$c_0 = a + \frac{B_r(a - c_{Tr}) + B_i c_{Ti}}{m[(a - c_{Tr})^2 + c_{Ti}^2]}, \tag{47}$$

$$\epsilon = \frac{B_i(a - c_{Tr}) - B_r c_{Ti}}{m[(a - c_{Tr})^2 + c_{Ti}^2]}. \tag{48}$$

From the second of (45) it follows that ϵ needs be at least as large as c_{Ti}; otherwise the root b will be unstable. Putting $\epsilon = c_{Ti}$ in (48) and varying a, we find that the maximum allowable m is

$$m_{\max} = (B_r/2c_{Ti}^2)\{(1 + \sigma^2)^{\frac{1}{2}} - 1\}, \tag{49}$$

where $\sigma = B_i/B_r = A_i/A_r$, which occurs for

$$a = c_{Tr} + c_{Ti}\{\sigma^{-1} + (1 + \sigma^{-2})^{\frac{1}{2}}\}. \tag{50}$$

Introducing these values into (47), we obtain the following optimum value for c_0:

$$c_0 = c_{Tr} + 2c_{Ti}\{\sigma^{-1} + (1 + \sigma^{-2})^{\frac{1}{2}}\}. \tag{51}$$

From (45) it then follows that $b = a$, i.e. a is a double root. Since c_{Ti} is generally very small, it may in practice often be impossible to find a flexible material with such a small damping that $\epsilon = c_{Ti}$. Hence in many practical cases ϵ will be given by the lowest value one can achieve. One then finds that the optimum value of a is again given by (50), but instead of (49) and (51) one obtains

$$m_{\max} = \frac{B_r}{2c_{Ti}\epsilon}\{(1 + \sigma^2)^{\frac{1}{2}} - 1\}, \tag{49a}$$

and

$$c_0 = c_{Tr} + (c_{Ti} + \epsilon)\{\sigma^{-1} + (1 + \sigma^{-2})^{\frac{1}{2}}\}, \tag{51a}$$

respectively. Hence the maximum allowable mass is inversely proportional to the damping. In this case the second root b is damped with its real part given by (45).

These results can be given a simple graphical interpretation. In the complex plane, (42) approximates Y_0 by a straight line and Y by a circle with radius $r = (md)^{-1}$ and centre at $Y_r = r$. One can easily show that, in the optimum case, Y is tangent to Y_0 at $c = a$. Hence it is easy to find the optimum Y by constructing the circle tangent to Y_0 with its centre on the real axis. The requirement that the point of tangency should correspond to the same value of c for both Y and Y_0 gives the necessary relation that fixes m and c_0 for a given d. It is suggested that this graphical method gives very nearly the optimum wall properties also with Y and Y_0 given by their exact expressions. The minimum value of d is that for which $\partial(\Delta Y)/\partial c = 0$ at a, since then a becomes a double root. Results of such constructions are shown in figure 7 for $R = 3000$ and two values of α, namely $\alpha = 0{\cdot}4$ and $\alpha = 0{\cdot}8$. The optimum values of m and c_0 thus obtained are plotted versus d. Evidently the damping must be very low unless a very light wall is used. Also the most unstable Tollmien–Schlichting waves with wave-numbers of order unity are relatively easy to stabilize compared to those of lower wave-numbers. In fact, with a flexible surface, the most difficult ones to stabilize are those with wave-numbers below those for the unstable region in the rigid-wall case. The reason for this is that the flexible wall tends to shift the unstable region to lower α, as was found by Benjamin (1960).

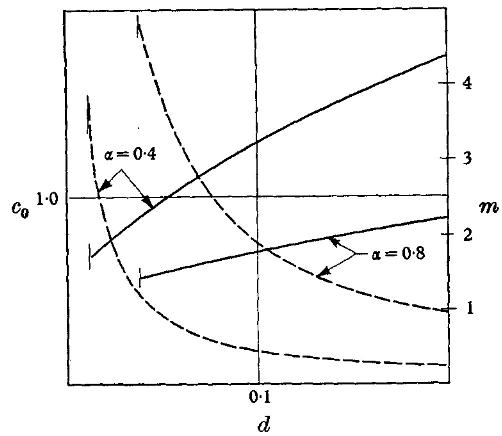

FIGURE 7. Optimum surface properties determined for $R = 3000$ as function of the damping coefficient d. ——, c_0; – – – –, m.

The dependence of the wall parameters on α determined by the method described above could probably in most cases not be reproduced by any material wall, so that the actual design of a suitable flexible wall for stabilizing all wave-numbers would be based on a compromise between the requirements for different wave-numbers. Furthermore, the present method gives no information as to whether stability will exist for Reynolds numbers away from the design value. In fact, for the case of minimum damping, instability would almost always occur if the Reynolds number were changed from its design point. Also, change of any one of the parameters for the flexible wall would cause instability.

7. The role of damping

We will now study the special role that is played by the damping in the flexible surface. For this purpose, consider the surface to be subjected to a forced oscillation in a travelling-wave mode with constant amplitude, such that the normal velocity is $v_1 = \hat{v} \exp [i\alpha(x-ct)]$. The non-dimensional pressure required for this is $\Delta Z v_1$, where the mechanical wave impedance $\Delta Z = \Delta Z_r + i\Delta Z_i$ of the system is the difference between the actual surface impedance and that required to maintain neutrally stable waves, i.e.

$$\Delta Z = Y^{-1} - Y_0^{-1} = i\alpha m\{(c_0^2/c) - c - i(d/\alpha)\} - Y_0^{-1}, \tag{52}$$

where the expression (34) for Y has been used. The imaginary (reactance) part of ΔZ represents the pressure component that is in phase with the surface deformation, whereas the real (resistive) part gives the out-of-phase component. At the real eigenvalue $c = a$, both the real and imaginary parts of ΔZ vanish. Suppose now that the damping ratio d in the layer is increased by a small amount Δd. To sustain the oscillation at constant amplitude will then require the mean power transfer per unit length of

$$\bar{E} = \tfrac{1}{2} m \Delta d \, |\hat{v}|^2. \tag{53}$$

The eigenvalue will change to $a + \Delta c$, where in the first approximation

$$\Delta c = \Delta c_r + i \Delta c_i = -m \Delta d / (\partial \Delta Z / \partial c)_{c=a}. \tag{54}$$

The imaginary part of Δc will be positive or negative depending on whether the imaginary part of $(\partial \Delta Z/\partial c)_{c=a}$ is greater or less than zero. From (52) we find that

$$\operatorname{Im}\{(\partial \Delta Z/\partial c)_{c=a}\} = -\alpha m\{1 + (c_0^2/a^2)\} - \operatorname{Im}\{\alpha^2 m^2 [(c_0^2/a) - a - (id/\alpha)]^2 (\partial Y_0/\partial c)_{c=a}\}, \tag{55}$$

since $Y_0 = Y$ for $c = a$. The imaginary part of $\partial Y_0/\partial c$ will generally be negative, so that the second term will be positive (assuming d to be small). Hence the sign of (55) depends on whether the first or second term dominate. For class B waves (for which the wave speed is close to c_0), the second term becomes small so that $\operatorname{Im}\{\partial \Delta Z/\partial c\} < 0$ and hence $\Delta c_i < 0$, i.e. the root is stable. For class A waves, on the other hand, the second term will dominate, making $\operatorname{Im}\{\partial \Delta Z/\partial c\} > 0$ and hence $\Delta c_i > 0$, i.e. the root unstable. Thus we find that an increase in the damping will stabilize class B waves but destabilize class A waves, in accordance with Benjamin's (1960) observation. For both types of waves, however, the power required to sustain a wave of constant amplitude increases with the damping. This property, which turns out to be special to waves travelling with a speed that is subsonic with respect to the fluid and is less than the free-stream speed, can most easily be studied by considering the case of potential flow, for which the characteristic equation (52) simplifies to

$$i\alpha m\left(\frac{c_0^2}{c} - c - i\frac{d}{\alpha}\right) - \frac{i(1-c)^2}{c} = 0. \tag{56}$$

For $d = 0$ this is exactly equivalent to the equation employed by Benjamin (1960) for studying Kelvin–Helmholtz instability. The flow causes a negative pressure that is in phase with the deformation and proportional to the wave-number and the square of the difference between the flow speed and the wave speed. The wave speed adjusts itself to make the induced pressure balance the 'effective stiffness' (stiffness − |inertial reaction|) of the flexible surface. Provided the stiffness is sufficiently high there will be two values a_r and b_r of the wave speed for which this is possible (see figure 8). Lowering of the stiffness will cause a_r to increase and b_r to decrease.

For very low wall-stiffness there will be no real value of c for which the effective stiffness balances the induced pressure. This case is illustrated by the broken line in figure 8. No neutrally stable wave then can exist, but instead Kelvin–Helmholtz instability will occur. Thus, the lowest allowable stiffness required to avoid instability is that for which a_r and b_r coalesce, and it is immediately apparent from the figure why Kelvin–Helmholtz instability never can occur for $c_0 \geqslant 1$ as Benjamin's (1960) result shows.

Consider now the case with damping. Solution of (56) gives for the two roots

$$a = a_r + ia_i = (1+\alpha m)^{-1}\{1+\tfrac{1}{2}imd-(1-q-imd)^{\frac{1}{2}}\}, \tag{57}$$

$$b = b_r + ib_i = (1+\alpha m)^{-1}\{1-\tfrac{1}{2}imd+(1-q-imd)^{\frac{1}{2}}\}, \tag{58}$$

where

$$q = (1-\alpha mc_0^2)(1+\alpha m)+\tfrac{1}{4}m^2d^2. \tag{59}$$

Three different cases may be distinguished: namely, when $q < 0$, $0 < q < 1$, and $q > 1$. In the first, the surface stiffness is so high that the wave speed for the a-wave (equation (57)) is negative and both waves are damped. (Note that m

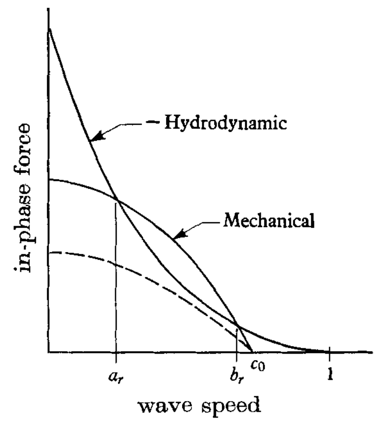

FIGURE 8. Balance of in-phase forces.

and c_0 generally are functions of α, and that, for low α, mc_0^2 is proportional to α^{-2}, so that q is always negative in the limit of vanishing α.) In the second case, both waves have a positive wave speed, the slowest wave being unstable and the the other stable. This corresponds to the case illustrated by the solid curve in figure 8. In the third case, which corresponds directly to the low-stiffness case illustrated by the broken curve in figure 8, the square-root term in (57) and (58) will have a large imaginary part, i.e. a violent instability of the Kelvin–Helmholtz type will occur. Evidently the lowest allowable stiffness for complete stability in the region of small wave-number is not determined by the Kelvin–Helmholtz instability condition as shown by Benjamin (1960) for the case $d = 0$, but rather by the more restrictive condition that $q < 0$ in the whole region.

The roots a and b in the simplified problem correspond directly to the class A and class B types of waves, respectively, in the full viscous problem. Evidently the destabilizing effect of damping on class A waves is not essentially associated with the fluid viscosity. It should therefore be possible to obtain a physical explanation of this property by studying the simplified problem in more detail.

Let us assume that a neutrally stable wave has been set up in a membrane without damping. Travelling with the wave there will be a pressure distribution in phase with the wave that balances exactly the 'effective stiffness' of the membrane. Assume now that damping is introduced, for example, by exposing the lower surface of the membrane to a viscous fluid. The damping will cause an out-of-phase pressure distribution acting on the lower membrane surface as illustrated in figure 9.

From the figure it is evident that this pressure distribution should have the effect of a second-order 'brake' on the travelling wave, and hence tend to slow it down. If the in-phase restoring force increases with c, as is the case for class A waves, then the force exerted by the damping will tend to lower the wave velocity into a region of c for which the elastic force is insufficient to counteract the sum of hydrodynamic and inertial forces acting on the membrane. However, since these are always in phase with the deformation for waves of constant amplitude,

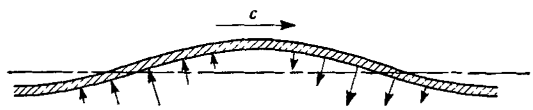

FIGURE 9. The retarding effect of damping.

the amplitude must start changing in order to effect a balance of the out-of-phase forces. Because there is an insufficient elastic restoring force at the slightly lower wave speed, the wave will diverge. For class B waves, on the other hand, the retarding effect of the damping on the wave will tend to move it to a wave-speed region where the net restoring force is positive and the wave amplitude will attenuate (as a damped oscillation).

The different effect of damping in the two cases becomes even clearer when one considers the energy associated with a wave. The disturbances created in the flow by the travelling wave in the wall will cause a change in the kinetic energy of the fluid. Since this change is of second order in the wave amplitude, it is necessary to include all second-order contributions like, for example, that emanating from the use of $y = \mathrm{Re}\{a \exp[i\alpha(x-ct)]\}$ instead of $y = 0$ as the lower boundary of the fluid. One then finds that the mean change in kinetic energy per unit streamwise length is given to second order by

$$\Delta T = -\tfrac{1}{4}\alpha a^2(1-c^2). \tag{60}$$

(This result is given in non-dimensional form.) Hence, for $c < 1$ there is a loss of kinetic energy in the fluid associated with the wave. Some of this energy has gone into kinetic and elastic energy in the membrane. Adding these contributions, we find that the total energy change associated with the wave in the membrane and the fluid is

$$\Delta W = \tfrac{1}{4}\alpha a^2[\alpha m(c_0^2+c^2)-(1-c^2)]. \tag{61}$$

Using the definition of the impedance of the wall in the presence of the stream, this expression can immediately be identified with

$$\Delta W = -\mathrm{Im}\{c^2(\partial \Delta Z/\partial c)\}\,\tfrac{1}{4}\alpha a^2. \tag{62}$$

Indeed, one can obtain this result without investigating the flow and the membrane separately. Consider the energy required to bring the velocity amplitude $\hat{v}(t)$ (assumed as real) up slowly from zero a final value $\hat{v}_0$. The pressure amplitude required to be applied on the lower surface of the flexible wall is, to first order,

$$\hat{p} = \mathrm{Re}\{\hat{v}(t)\,\Delta Z + \dot{\hat{v}}(t)\,(i/\alpha)\,(\partial \Delta Z/\partial c)\}, \tag{63}$$

the last term being obtained by a first-order analytical continuation of c into the complex plane. The total energy supplied to the system during the process is

$$\int_0^{t_0} \hat{p}(t)\,\hat{v}(t)\,dt.$$

Averaging over x and using (63) for $\hat{p}$ gives

$$W = \tfrac{1}{2}\,\mathrm{Re}\{\Delta Z\}\int_0^{t_0} \hat{v}^2\,dt - \frac{\hat{v}_0^2}{4\alpha}\,\mathrm{Im}\left\{\frac{\partial \Delta Z}{\partial c}\right\}. \tag{64}$$

The first term may be interpreted as the energy dissipated during the process, whereas the second term represents the potential energy stored in the system. Hence, by substituting $\alpha^2 c^2 a^2$ for $\hat{v}_0^2$, (62) follows. The result (64) does not necessarily hold in the case of a viscous flow, since the energy dissipated in the fluid may contain a part proportional to $d\hat{v}/dt$. (To calculate this one would need to

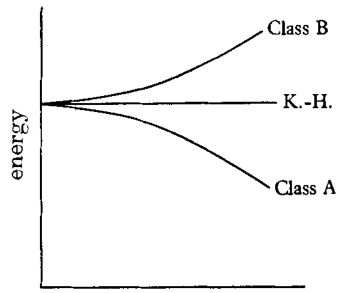

FIGURE 10. Variation of total kinetic and elastic energy with amplitude for the three different classes of waves.

consider also second-order terms in the equations of motion.) However, this is unlikely to affect the discussion below, which is based on the assumption that (62) gives correctly the sign of the stored energy in the viscous case also. Since $\mathrm{Im}\{\partial \Delta Z/\partial c\}$ is positive for class A waves, negative for class B waves and zero for Kelvin–Helmholtz instability, ΔW would vary with amplitude in the manner illustrated in figure 10. Thus, for class A waves ΔW is always negative, and further dissipation of energy from the system, through increased wall damping, will only make the wave amplitude increase to compensate for the lowered energy level. Class B waves, on the other hand, have a positive ΔW and therefore behave in the 'normal' way. For the Kelvin–Helmholtz instability, finally, the total energy level does not change with changing amplitude; there is only a redistribution of energy from kinetic energy in the fluid to elastic energy in the wall, and any increase in the wall damping will consequently have a negligible effect on the disturbance amplitude.

Returning now to the complete viscous problem, there will always be regions of α and c for which the elastic restoring force of the wall will be insufficient to balance the hydrodynamic force, since there are combinations for which Y_0 is close to zero, i.e. Z_0 very large. Thus, this is equivalent to the second case in the potential-flow solution above, and hence class A waves will always be possible.

In applying the energy considerations above, it is necessary to include in the full problem two further mechanisms of energy transfer, namely through the action of viscosity and Reynolds stresses, respectively. Through the first one, mechanical energy is dissipated into heat, and viscosity thus has an effect very much similar to that of the wall damping. Thus we arrive at a new explanation of the role of viscosity in the rigid-wall case, namely that it provides the mechanism whereby the energy required to make the Tollmien–Schlichting waves unstable is removed. The Reynolds stresses generally tend to transfer energy from the free stream to the disturbance.† This energy transfer increases with increased wave velocity and increased curvature of the boundary-layer profile. It is then clear how the present method of boundary-layer stabilization works. The energy required to attenuate the class A waves is supplied by the Reynolds stresses. By decreasing the wall stiffness, the wave speed is increased and thereby also the rate at which energy is being transmitted by the Reynolds stresses. The lower the damping in the flexible wall, the less the wave speed needs to be increased to achieve stabilization. On the other hand, the damping must be large enough so that the total effective damping for the class B waves is positive.

8. Conclusions

The method used in the present analysis differs from that commonly employed for stability problems in that the problem is first formulated as a direct boundary-value problem, namely that of calculating the wall admittance required to maintain a given neutrality stable wave. Comparison of this admittance to that of a given wall results in a characteristic equation whose solution yields the curve for neutral stability. In addition to simplifying the analysis somewhat, the method also leads to a systematic physical interpretation of the general effects of the flexible surface. The characteristic equation derived in the present paper differs from that given in Benjamin's (1960) analysis by terms involving the (generally small) quantity $\lambda(c)$ arising from the use of a slightly more accurate version of the viscous solution. In the present paper, the characteristic equation for the flexible-wall problem is thus brought up to the same state of development as the currently used equation for the rigid-wall case (see, for example, Lin 1955), to which the present equation reduces as the wall flexibility vanishes. For a flexible wall with damping, the correction terms involving λ tend to be slightly more important than in the rigid-wall case; however, they are still small and can probably be neglected in most practical cases, at least for a Blasius profile.

To solve the characteristic equation, a relatively simple graphical procedure was devised, which could also be used with measured properties of the elastic wall. Since for the wall with damping several regions of instability can occur, it

† At first sight it may seem paradoxical that the Reynolds stresses can change the *total* energy level of the flow since the net effect of energy transfer from one part of the flow to another obviously would be zero. However, upon closer examination one finds that the Reynolds stresses cause an ultimate decrease of viscous energy dissipation (through the action of the second-order mean-flow distortion), which in the case of neutral disturbances is equal to the 'energy transmitted by Reynolds stresses'. Since the latter phraseology is an accepted one in the literature on hydrodynamic stability, we have retained it here.

was necessary to develop a method whereby one can determine which side of a neutral curve is unstable. The graphical method proposed is based on the assumption that the amplification rates are generally small.

The main effort in the present paper was expended on the study of the effects of a wall with internal damping. This subject was treated only qualitatively in Benjamin's (1960) paper. For simplicity we assumed that the mechanical properties of the flexible wall could be fully described by three parameters, namely the mass coefficient, free-surface (Rayleigh) wave speed, and the damping. Even for such a rudimentary wall representation, the problem of determining the combination of these parameters giving the best over-all effect is quite difficult. According to the theory, stabilization can always be achieved by a wall of sufficient flexibility and lightness, provided all the different modes of instability can be suppressed. For practical reasons one would therefore like to find the combination of parameters that allows the use of the heaviest and stiffest surface. The graphical method developed in the present paper produces such a combination for each wave-number considered. The design of any material wall for operation at given Reynolds number has, of course, to be based on a compromise between the requirements for various wave-numbers and, for such an over-all design, the present method may be of limited practical value. However, it does produce some useful information; in particular it indicates that the damping should be very low for best results.

The effects of damping were discussed to some length. The remarkable result that wall damping tends to destabilize class A waves was found to have an interesting explanation. It was shown that class A waves are energy deficient in the sense that the total kinetic and elastic energy of the system decreases with increasing wave amplitude. Hence any further energy dissipation through wall damping will only make the amplitude increase to compensate for the lowered energy level. This unexpected property was discovered by considering the very simplified problem of the stability of a flexible wall in potential flow, which was essentially the problem studied by Miles (1956) in a paper on panel flutter. However, Miles only considered non-dissipative panels in which case the only instability that can occur is of the Kelvin–Helmholtz type. For such an instability the energy content is constant and damping will have very little effect on it. The fact that damping can introduce a new mode of mild panel instability has apparently been overlooked in the literature, although some calculations have indicated that damping occasionally can be destabilizing. This mode of instability will occur at lower speeds than the Kelvin–Helmholtz one, namely as soon as the dynamic pressure becomes high enough to sustain a steady waviness of the panel, i.e. at the speed of 'static divergence'.

We may conjecture that since the Tollmien–Schlichting waves are of the class A type, they are associated with a decrease in the total kinetic energy of the flow in the boundary layer. Hence they can only be stabilized by a mechanism of 'negative damping' which is supplied by the Reynolds stresses feeding energy from the free stream to the disturbance. In the rigid-wall case this negative damping can be increased by giving the free stream outside the boundary layer a positive velocity gradient, in which case the magnitude of the curvature of the boundary-layer velocity profile at the critical layer increases and hence the Reynolds stresses. In the present method of boundary-layer stabilization, the phase speed of the Tollmien–Schlichting wave is increased through the introduction of wall flexibility and thereby the Reynolds stresses. The greater the damping in the wall, the more the phase speed must be increased through increased wall flexibility to make the total damping (internal damping less the effect of Reynolds stresses) negative and hence stabilize the class A waves. If the wall damping is not too small, the total damping at the phase speed for the class B waves will be positive, and hence both types of waves will be damped. Evidently the selection of the best wall damping is rather critical, as is also apparent from the numerical example shown.

The limited number of numerical calculations presented seems to indicate that the increases in critical Reynolds number obtainable with flexible surfaces of rather large flexibility are quite modest. It seems therefore unlikely that the reported success of Krämer's (1960 *a*, *b*) experiments could be explained on the basis of the simple stability theory alone. Furthermore, he seems to have obtained the best results with moderately high wall damping, contrary to the present analysis which shows that the damping ought to be very low. One is therefore led to look for other explanations of the observed effects. The two most likely alternative explanations are that the flexible surface either modifies some later stages in the process of transition, or that it has an effect on the fully developed turbulent boundary layer. The further exploration of these ideas is unfortunately hampered by the incomplete understanding of both the phenomenon of transition and the turbulent boundary layer. However, the first of these alternatives is supported by Benjamin's (1960) observation that the flexible surface tends to cancel the wall friction-layer and hence make the disturbance mainly inviscid. To gain some quantitative insight into this phenomenon, we may write (18) as follows:

$$\phi = \Phi_w(\Phi/\Phi_w - C\phi_3/\phi_{3w}), \tag{65}$$

where

$$C = \frac{c\Phi'_w/\Phi_w + U'_w}{c\phi'_{3w}/\phi_{3w} + U'_w}. \tag{66}$$

By introducing equations (20)–(26) and solving (31) for $u+iv$ in terms of $\mathscr{F}$ and Y, we obtain

$$C = \frac{\mathscr{F}-1}{\mathscr{F}-1+iU'_w Y/\alpha}. \tag{67}$$

For a rigid wall, obviously $C = 1$, since the viscous solution ϕ_3 must cancel the inviscid one Φ at the wall. As an example, figure 11 shows C for the case of the flexible wall considered in figure 4. Evidently the flexible wall has cancelled about 80 % of the viscous solution. (Note that this particular wall has an unfavourable effect on the critical Reynolds number.) The flexibility also generally causes the unstable region to move towards smaller wave-numbers. Both these effects tend to give the instability more the character of 'panel instability' than 'boundary-layer instability'; in particular the vorticity released in the flow by the disturbance (which probably originates to a large extent from the wall friction-layer) will decrease.

Some obvious and straightforward extensions of the present analysis are possible. One is to consider waves that are oblique to the free stream. In the present case Squire's (1933) transformation is not directly applicable, since the surface flexibility scales as the square of the velocity component in the direction of the wave and therefore becomes less effective for oblique waves. Another possible extension is to include the tangential deformation of the surface. This

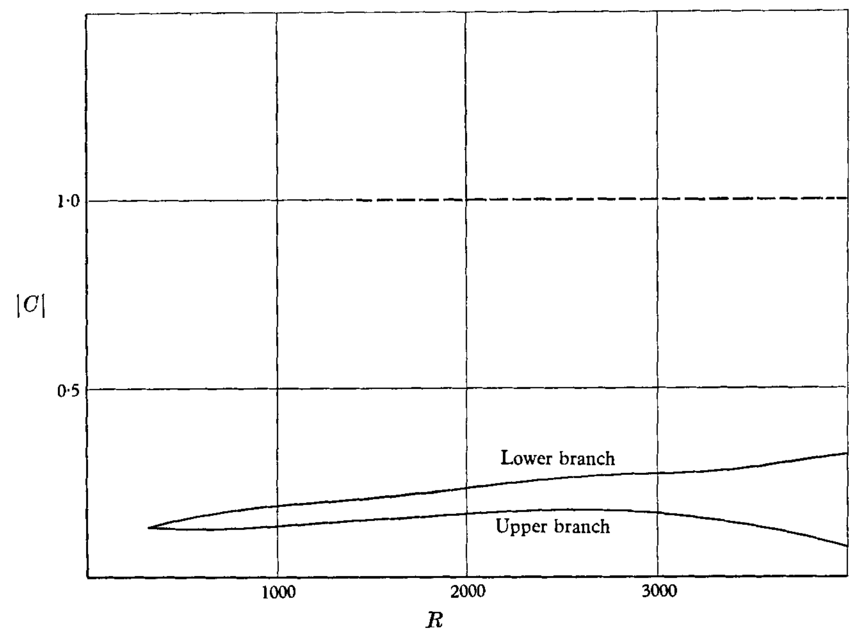

FIGURE 11. Ratio of 'viscous' to 'non-viscous' solution at the wall for the case considered in figure 4. ----, Rigid wall; ——, flexible wall.

was done for a non-dissipative surface in Nonweiler's (1961) paper. One should note in this connexion that the shear fluctuations at large Reynolds numbers are terms of higher order and should therefore be neglected for consistency with the asymptotic solution. However, the deformation normal to the surface may cause tangential deformations that may affect the stability. A third, somewhat more complicated extension is to make the corresponding analysis for compressible flow. Such preliminary calculations have been carried out recently by Linebarger (1961).

I am indebted to Dr T. Brooke Benjamin for many helpful discussions of the problem and his constructive criticism of a preliminary version of the present paper. His extended visit to Mass. Inst. of Technology during August 1961 was supported by the Office of Naval Research through an arrangement with Prof. C. C. Lin. This research was sponsored in part by the Air Force Office of Scientific Research under Contract AF 49 (638)–933.

REFERENCES

Benjamin, T. Brooke 1959 Shearing flow over a wavy boundary. *J. Fluid Mech.* **6**, 161.

Benjamin, T. Brooke 1960 Effects of a flexible boundary on hydrodynamic stability. *J. Fluid Mech.* **9**, 513.

Betchov, R. 1959 Simplified analysis of boundary-layer oscillations. *Douglas Aircraft Company Report*, no. ES-29174.

Boggs, F. W. & Tokita, N. 1960 A theory of the stability of laminar flow along compliant plates. Paper presented at the *Third Symp. on Naval Hydrodynamics, Scheveningen, Holland, September*, 1960.

Hains, F. D. & Price, J. F. 1961 Effects of flexible walls on the stability of plane Poiseulle flow. Paper presented at the 1961 *Annual Meeting of the Amer. Phys. Soc. February* 1961.

Krämer, M. O. 1960*a* Reader's Forum. *J. Aero/Space Sci.* **27**, 68.

Krämer, M. O. 1960*b* Boundary-layer stabilization by distributed damping. *J. Amer. Soc. Nav. Engrs*, **72**, 25.

Lees, L. 1947 The stability of the laminar boundary layer in a compressible fluid. *NACA Rep.* no. 876.

Lin, C. C. 1945 On the stability of two-dimensional parallel flows. Parts I, II and III. *Quart. Appl. Math.* **3**, 117, 218, 277.

Lin, C. C. 1955 *The Theory of Hydrodynamic Stability*. Cambridge University Press.

Linebarger, J. H. 1961 On the stability of a laminar boundary layer over a flexible surface in a compressible fluid, S.M. Thesis, Dept. Aeronautics and Astronautics, M.I.T.

Miles, J. W. 1956 On the aerodynamic instability of thin panels. *J. Aero. Sci.* **23**, 77.

Miles, J. W. 1960 The hydrodynamic stability of a thin film of liquid in uniform shearing motion. *J. Fluid Mech.* **8**, 593.

Nonweiler, T. 1961 Qualitative solutions of the stability equation for a boundary layer in contact with various forms of flexible surface. *A.R.C. Rep.* no. 22, 670.

Schlichting, H. 1960 *Boundary Layer Theory*, 4th ed. New York: McGraw-Hill.

Squire, H. B. 1933 On the stability of the three-dimensional disturbances of viscous flow between parallel walls. *Proc. Roy. Soc.* A, **142**, 621.

Tollmien, W. 1947 Asymptotische Integration der Störungsdifferentialgleichung ebener laminarer Strömungen bei hohen Reynoldschen Zahlen. *Z. angew. Math. Mech.* **25/27**, 33, 70.